Electrochemistry
The Electrochemical Society of Japan
Received: March 7, 2023
Accepted: March 11, 2023
Published online: March 15, 2023
Issued: April 18, 2023
https://doi.org/10.5796/electrochemistry.23-00025
https://doi.org/10.50892/data.electrochemistry.22266718
Note
Electrochemistry, 91(4), 047003 (2023)

Effects of Ion Fraction in an Inorganic Ionic Liquid Electrolyte on Performance of Intermediate-Temperature Operating Sodium-Sulfur Batteries

Di WANG,[a,§] Jinkwang HWANG,[a,§§] Keigo KUBOTA,[b,§§] Kazuhiko MATSUMOTO,[a,*,§§] and Rika HAGIWARA[a,§§§]

[a] Graduate School of Energy Science, Kyoto University, Yoshida, Sakyo-ku, Kyoto 606-8501, Japan
[b] Department of Energy and Environment, Research Institute of Electrochemical Energy, National Institute of Advanced Industrial Science and Technology (AIST), 1-8-31 Midorigaoka, Ikeda, Osaka 563-8577, Japan

* Corresponding author: k-matsumoto@energy.kyoto-u.ac.jp

ABSTRACT

Sodium-sulfur (Na-S) batteries are promising energy storage systems for renewable energy sources which redeem an intermittent energy source. This study reports the effects of the $Na[SO_3CF_3]$ fraction in an inorganic $Na[SO_3CF_3]$-$Cs[N(SO_2CF_3)_2]$ ionic liquid electrolyte ($x(Na[SO_3CF_3])$ = 0.2, 0.3, and 0.4) on the performance of Na-S batteries. Measurements of physicochemical and electrochemical properties demonstrated that decrease in the $Na[SO_3CF_3]$ fraction decreases viscosity and increases ionic conductivity and the solubility of polysulfides into the ionic liquid, which contributes to the enhanced capacity in the low potential region during discharging.

Keywords : Electrolyte, Sodium-sulfur Batteries, Inorganic Ionic Liquid, Polysulfide Solubility

1. Introduction

Energy storage devices are critical in the contemporary society from small electric devices to large-scale energy storage. In terms of the power grid use, they enable integration of intermittent renewable energy sources like solar and wind powers.[1] Because of their high energy density, extended cycleability, and resource sustainability, sodium-sulfur (Na-S) battery is one of the most practical energy storage technologies.[2] Traditional Na-S batteries require a high working temperature over 573 K to operate with a sufficiently low interfacial resistance, including the use of liquified Na_2S_x (S_x^{2-} = polysulfide anion) and employ a beta alumina solid electrolyte (BASE) to prevent the so-called shuttle effect. The shuttle effect refers to the transport of S_x^{2-} from the positive electrode to the negative electrode, where they interact directly with the negative electrode active materials (molten Na metal). In other words, BASE can block S_x^{2-} by selectively conducting Na^+. However, the operation of Na-S batteries at high temperatures poses certain disadvantages such as energy loss and material selectivity. Most crucially, to keep the reactant liquid above 573 K, the discharged product is confined to Na_2S_3 with a capacity of 557 mAh $(g\text{-}S)^{-1}$ or 33.3 % of utilization of the theoretical capacity.[3]

To address these concerns, previous studies investigated the feasibility of Na-S batteries at room temperature by using liquid electrolytes as the reaction media.[4] This approach could make use of a broader range of polysulfides, such as Na_2S_x (where $x < 3$), but organic electrolytes used at room temperature generally exhibit flammability, instability, and vulnerability of Na dendrites and reintroduced the shuttle effect problem because of the lack of BASE.[5–8] Although there are also many attempts to use solid-state electrolytes and polymer gel electrolytes, they are still in their infancy and have drawbacks such as poor interfacial contact and unstable cycling performance.[9]

One possible solution to these problems is the operation of Na-S batteries at intermediate temperatures (~423 K). Such operation is feasible to combine the advantages of BASE and liquid electrolytes; BASE inhibits the shuttle effect of S_x^{2-} and the liquid electrolyte in the positive-electrode compartment facilely enables dissolution of polysulfides without melting (thus increases the sulfur usage) and Na^+ conduction at the solid-liquid interface.[10–15] The use of ionic liquid electrolytes for sodium secondary batteries are widely investigated owing to their unique properties.[16,17] A previous research revealed that the Na[OTf]-Cs[TFSA] ($[SO_3CF_3]^-$ = $[OTf]^-$ = trifluoromethanesulfonate and $[N(SO_2CF_3)_2]^-$ = $[TFSA]^-$ = bis(trifluoromethanesulfonyl)amide) inorganic ionic liquid system can be successfully used as an liquid electrolyte in such a solid-liquid dual electrolyte for Na-S batteries owing to their low flammability, volatility, and high electrochemical and thermal stabilities.[15] However, the effects of Na[OTf] fraction on performance of this battery are not investigated in details, although the phase diagram was constructed in the Na[OTf] fraction range from 0 to 0.8. Moreover, the Na[OTf] fraction can dually affect the performance; the Na^+ concentration is directly related to the Na^+ transport properties and electrode reaction and the $[OTf]^-$ fraction influences the solubility of polysulfides into the electrolyte owing to its high donor number.[15] In this paper, the physicochemical and electrochemical properties of the Na[OTf]-Cs[TFSA] system are investigated to elucidate the effects of the Na[OTf] fraction on the Na-S battery performance.

2. Experimental

A vacuum line made of stainless steel, borosilicate glass,

§ECSJ Student Member
§§ECSJ Active Member
§§§ECSJ Fellow
D. Wang orcid.org/0000-0002-4816-9855
J. Hwang orcid.org/0000-0003-4800-3158
K. Kubota orcid.org/0000-0002-0536-129X
K. Matsumoto orcid.org/0000-0002-0770-9210
R. Hagiwara orcid.org/0000-0002-7234-3980

poly(tetrafluoroethylene), and poly(tetrafluoroethylene-co-perfluoro(alkylvinyl)ether) (PFA) was used to dry materials. Nonvolatile materials were handled in a glove box under a dry Ar environment (H_2O < 1 ppm, O_2 < 1 ppm). Sulfur (Wako Pure Chemical, purity > 98.0 %) was dried for one day in a PFA container at 393 K under vacuum. To avoid sublimation outside the container, the upper half of the container was cooled by a blower. The Na[OTf] (Sigma-Aldrich, purity > 98 %) salt was vacuum-dried at 373 K for 3 days. The Cs[TFSA] (Morita Chemical, purity > 99.0 %) salt was dissolved in anhydrous ethanol to generate a saturated solution, which was subsequently recrystallized by adding an equivalent volume of trifluorotoluene as the lean solvent. The resultant white solid was vacuum-dried at 373 K for 3 days. The component salts were blended in the desired molar ratios, heated above their melting points, and repeatedly agitated to achieve a homogenous Na[OTf]-Cs[TFSA] mixture.

Ionic conductivities of the electrolytes were determined by AC impedance spectroscopy with a 10 mV AC perturbation (Hokuto Denko, HZ-Pro). The sample was sealed in a cell with two Pt black electrodes (Radiometer Analytical). The cell constant was calibrated with the KCl standard solution. A digital viscometer (Brookfield Engineering Laboratories, DV1MLVTJ0+HT-110115ADP) was used to measure viscosities. Densities of the samples were obtained by measuring the volume of the electrolyte at a constant weight in a calibrated container during heating.

The galvanostatic charge-discharge behavior was investigated at 423 K. The obtained ionic liquid was combined with BASE (Ionotec, 24 mm diameter, 1 mm thickness) for the Na-S cell as previously reported.[15] The positive electrode was made of sulfur and carbon paper conducting material (Toray, TGP-H-120). Carbon paper and BASE were vacuum-dried for 3 days at 573 K. Molten sodium metal (Aldrich, purity 99.95 %) served as the negative electrode. Prior to the measurements, carbon paper was impregnated with the electrolytes under vacuum above their melting points. The positive electrode compartment was filled with sulfur powder and the carbon paper/electrolyte composite (typically 3 mg S in 300 mg electrolyte). The apparent area of the negative and positive electrodes was 0.785 cm^2. After assembly, the cell was heated to 423 K for 12 h to achieve the temperature equilibrium. Cut-off voltages of charge-discharge tests were set to 1.2–2.8 V, and currents were regulated at 0.1, 0.2, 0.5, 1.0, and 2.0 mA. The specific capacity was estimated using the weight of sulfur.

The solubility was visually compared by the depth of the color of the electrolyte containing excessive Na_2S_4 (the weight ratios of 16 mg/1000 mg-electrolyte) in the among Na[OTf]-Cs[TFSA] mixtures with different ratios. The test tube was tightly sealed in the Ar-filled glove box and heated at 423 K.

3. Results and Discussion

Figure 1 shows physicochemical properties of the Na[OTf]-Cs[TFSA] ionic liquids at three different ratios (Na[OTf] : Cs[TFSA] = 20 : 80, 30 : 70, and 40 : 60 mol%) (see Tables S1, S2, and S3 for the corresponding viscosity, ionic conductivity, and density data). These three ratios were selected by considering the previously determined phase diagram in terms of operating temperature (423 K) and Na^+ fraction.[15] It is observed that the viscosity (η) of the electrolyte increases with increasing the Na[OTf] fraction (Fig. 1a). For example, this trend is evident when the viscosities at 423 K are compared (61.5, 80.4, and 104 mPa s at 20, 30, and 40 mol% of Na[OTf], respectively). On the other hand, the ionic conductivity (σ) decreases with increasing the Na[OTf] fraction in the order of 8.22, 6.15, and 5.72 mS cm^{-1} at 20, 30, and 40 mol% of Na[OTf] at 423 K, respectively (Fig. 1b). Temperature (T) dependence of both the viscosities and conductivities follows the Vogel-Tammann-Fulcher (VTF) equation as shown in Eqs. 1 and 2 (see Tables 1 and 2 for the fitting parameters):

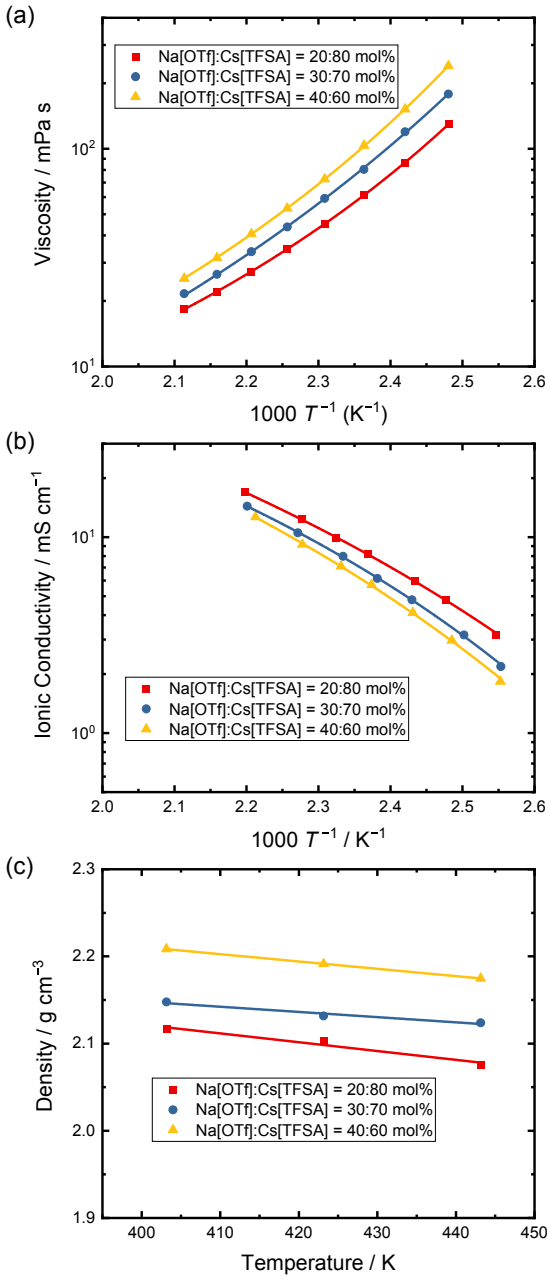

Figure 1. Temperature dependence of (a) viscosities, (b) ionic conductivities, and (c) densities for the Na[OTf]-Cs[TFSA] ionic liquid systems.

Table 1. VTF fitting parameters for the viscosities of the Na[OTf]-Cs[TFSA] systems. All the fitting data have $R^2 > 0.99$.

	Electrolytes		
	20 mol% Na[OTf]	30 mol% Na[OTf]	40 mol% Na[OTf]
A_η/mPa s $K^{-1/2}$	1.78×10^{-2}	5.76×10^{-3}	1.15×10^{-2}
B_η/K	7.80×10^{2}	1.19×10^{3}	9.65×10^{2}
$T_{0\eta}$/K	2.71×10^{2}	2.40×10^{2}	2.64×10^{2}

Table 2. VTF fitting parameters for ionic conductivities of the Na[OTf]-Cs[TFSA] systems. All the fitting data have $R^2 > 0.99$.

	Electrolytes		
	20 mol% Na[OTf]	30 mol% Na[OTf]	40 mol% Na[OTf]
A_σ/mS cm^{-1} K$^{1/2}$	3.08×10^4	1.97×10^4	3.86×10^4
B_σ/K	9.89×10^2	8.23×10^2	1.06×10^3
$T_{0\sigma}$/K	2.32×10^2	2.57×10^2	2.39×10^2

Table 3. Fitting parameters of densities for the Na[OTf]-Cs[TFSA] systems.

	Electrolytes		
	20 mol% Na[OTf]	30 mol% Na[OTf]	40 mol% Na[OTf]
A/g cm^{-3}	2.53	2.39	2.55
B/g cm^{-3} K^{-1}	-1.01×10^{-3}	-5.97×10^{-4}	-8.40×10^{-4}
R^2	>0.96	>0.96	>0.99

$$\eta(T) = A_\eta \sqrt{T} \exp\left(\frac{B_\eta}{T - T_{0\eta}}\right) \quad (1)$$

$$\sigma(T) = \frac{A_\sigma}{\sqrt{T}} \exp\left(-\frac{B_\sigma}{T - T_{0\sigma}}\right) \quad (2)$$

The VTF equation is often used to describe the temperature-dependent viscosity and ionic conductivity of glass-forming materials such as ionic liquids.[18–20] Here, A_σ, B_σ, A_η, and B_η are the fitting parameters, whereas $T_{0\eta}$ and $T_{0\sigma}$ represent ideal glass transition temperatures for viscosity and ionic conductivity, respectively. Temperature dependence of density (ρ) is fitted by the linear relation as illustrated in Fig. 1c according to Eq. 3 (see Table 3 for the fitting parameters).

$$\rho(T) = A + BT \quad (3)$$

Density decreases with increasing the Na[OTf] fraction because the large atomic mass of Cs^+ contributes more at the lower Na[OTf] fraction.

A previous research showed that all the Na_2S_x polysulfides are solid at 423 K and thus the electrochemical reactions must occur through the ionic liquid electrolyte by dissolving Na_2S_x.[13] However, previous reports revealed that low-order polysulfides (where $x < 4$) produced at lower voltages lead to significant voltage hysteresis below 1.9 V, which is due to the low solubility of these relevant polysulfides, precipitating in the electrolyte at 423 K.[13,15] Figure 2 compares the discharge-charge profiles of the Na-S cell with the Na[OTf]-Cs[TFSA] ionic liquid electrolytes at a current of 0.1 mA (electrode area: 0.785 cm^2). Although the conversion of high-order polysulfides above 1.6 V does not vary significantly with increasing the Na[OTf] ratio, the capacity below 1.6 V significantly decreases. This observation suggests that the conversion of Na_2S_3 to Na_2S_2 is lost when the Na[OTf] ratio is higher than 30 mol% (theoretical capacities of Na_2S_3 and Na_2S_2 are 557 and 836 mAh (g-S)$^{-1}$, respectively). This result indicates that the increased $[OTf]^-$ fraction does not simply improve sulfur utilization.

The Na[OTf] fraction also influences rate performance. Figure 3 presents comparison of the charge-discharge profiles during the rate performance test for the Na-S cells with the Na[OTf]-Cs[TFSA] ionic liquid electrolytes at 20 and 40 mol% Na[OTf]. The cell at 20 mol% Na[OTf] delivers a larger capacity than the cell at 40 mol% Na[OTf] at all the currents, indicating the higher utilization of low-order polysulfides at 20 mol% Na[OTf]. In contrast, the differences in capacity diminish with increasing currents, particularly at 2.0 mA, where high-order polysulfides contribute to the capacity.

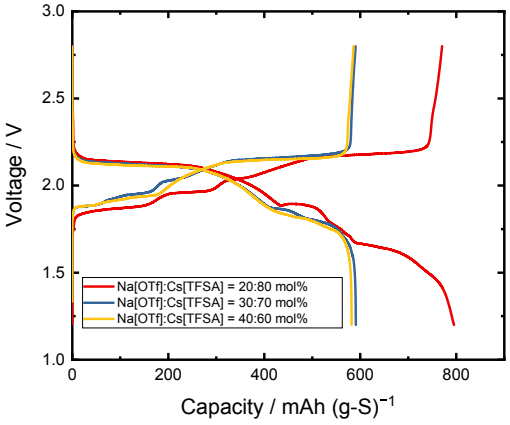

Figure 2. The discharge-charge profiles of the Na-S cells with the Na[OTf]-Cs[TFSA] ionic liquid electrolytes (Na[OTf] : Cs[TFSA] = 20 : 80, 30 : 70, and 40 : 60 in mol%) at 423 K. Current: 0.1 mA and electrode area: 0.785 cm^2. (The data of 20 mol% Na[OTf] was reproduced from previous report with permission.[15])

The solubility of Na_2S_x, which acts as a critical factor for the charge-discharge performance, was further explored through a visual solubility test. One of the representative polysulfides, Na_2S_4, was used for this test. As can be seen from Fig. S1, 20 mol% Na[OTf] electrolyte displays a darker yellow color than 40 mol% Na[OTf] electrolyte, indicating a higher presence of dissolved polysulfides.[21–23] This observation was in line with the electrochemical properties, as mentioned above that the high Na[OTf] fraction shows inferior discharge capacity.

4. Conclusion

This study examined the effects of Na[OTf] fraction on the Na-S battery performance using the Na[OTf]-Cs[TFSA] (Na[OTf]-Cs[TFSA] = 20 : 80, 30 : 70, and 40 : 60) ionic liquid electrolytes. The viscosity and ionic conductivity of the electrolyte increased and decreased with increasing the Na[OTf] fraction. Comparison of the charge-discharge profiles at different Na[OTf] fractions revealed that the conversion of high-order polysulfides to low-order polysulfides decreased from the case with 20 mol% Na[OTf] to 30 mol% and 40 mol% Na[OTf]. These results suggest that Na[OTf] does not simply improve sulfur utilization only by the increased solubilities of sulfur and polysulfide. In addition, the balance between the solubility and mass transfer ability is an important factor to improve the performance. The solubility test actually confirmed that the solubility of Na_2S_4 decreases with increasing the Na[OTf] fraction. However, in this study, the ratio of Na^+ and Cs^+ cations also changes, which can also affect the solubility of Na_2S_x. Thus, the role of individual cationic and anionic species in the solubility and electrochemical reactivity of polysulfides needs to be further investigated in the future.

Acknowledgment

This study was supported by Grant-in-Aid for Scientific Research (B) conducted through the support of the Japan Society for the Promotion of Science (JSPS, KAKENHI Grant Number 21H02047). One of the authors, Di Wang, thanks the China Scholarship Council (CSC) for the financial support.

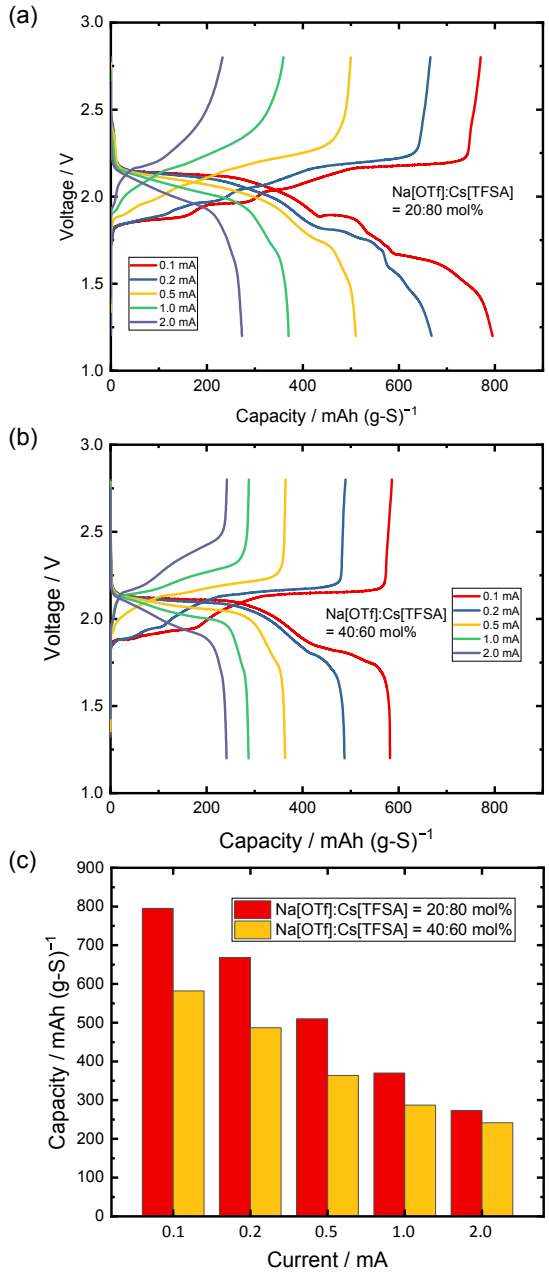

Figure 3. Comparison of the rate performance of the Na-S cells with the Na[OTf]-Cs[TFSA] ionic liquid electrolytes (Na[OTf] : Cs[TFSA] = 20 : 80 and 40 : 60 in mol%) at 423 K: (a) the charge and discharge profiles and (b) discharge capacities at different rates. (The data of 20 mol% Na[OTf] was reproduced from previous report with permission.[15])

CRediT Authorship Contribution Statement

Di Wang: Formal analysis (Lead), Investigation (Lead), Methodology (Equal), Visualization (Lead), Writing – original draft (Lead)

Jinkwang Hwang: Formal analysis (Supporting), Investigation (Supporting), Methodology (Equal), Supervision (Lead), Validation (Lead), Writing – original draft (Supporting), Writing – review & editing (Equal)

Keigo Kubota: Formal analysis (Supporting), Investigation (Supporting), Methodology (Supporting), Validation (Supporting), Writing – review & editing (Supporting)

Kazuhiko Matsumoto: Funding acquisition (Lead), Project administration (Lead), Resources (Equal), Supervision (Lead), Validation (Supporting), Writing – review & editing (Equal)

Rika Hagiwara: Data curation (Lead), Resources (Lead), Supervision (Supporting), Writing – review & editing (Supporting)

Data Availability Statement

The data that support the findings of this study are openly available under the terms of the designated Creative Commons License in J-STAGE Data listed in D1 of References.

Conflict of Interest

The authors declare no conflict of interest in the manuscript.

Funding

Japan Society for the Promotion of Science: 21H02047
China Sponsorship Council

References

D1. D. Wang, J. Hwang, K. Kubota, K. Matsumoto, and R. Hagiwara, *J-STAGE Data*, https://doi.org/10.50892/data.electrochemistry.22266718, (2023).
1. B. Dunn, H. Kamath, and J.-M. Tarascon, *Science*, **334**, 928 (2011).
2. T. Oshima, M. Kajita, and A. Okuno, *Int. J. Appl. Ceram. Technol.*, **1**, 269 (2004).
3. K. B. Hueso, V. Palomares, M. Armand, and T. Rojo, *Nano Res.*, **10**, 4082 (2017).
4. Y.-X. Wang, B. Zhang, W. Lai, Y. Xu, S.-L. Chou, H.-K. Liu, and S.-X. Dou, *Adv. Energy Mater.*, **7**, 1602829 (2017).
5. X. Hong, J. Mei, L. Wen, Y. Tong, A. J. Vasileff, L. Wang, J. Liang, Z. Sun, and S. X. Dou, *Adv. Mater.*, **31**, 1802822 (2019).
6. C. Arbizzani, G. Gabrielli, and M. Mastragostino, *J. Power Sources*, **196**, 4801 (2011).
7. T. Yim, M.-S. Park, J.-S. Yu, K. J. Kim, K. Y. Im, J.-H. Kim, G. Jeong, Y. N. Jo, S.-G. Woo, K. S. Kang, I. Lee, and Y.-J. Kim, *Electrochim. Acta*, **107**, 454 (2013).
8. Y.-X. Wang, W.-H. Lai, S.-L. Chou, H.-K. Liu, and S.-X. Dou, *Adv. Mater.*, **32**, 1903952 (2020).
9. M. S. Syali, D. Kumar, K. Mishra, and D. K. Kanchan, *Energy Storage Mater.*, **31**, 352 (2020).
10. X. Lu, B. W. Kirby, W. Xu, G. Li, J. Y. Kim, J. P. Lemmon, V. L. Sprenkle, and Z. Yang, *Energy Environ. Sci.*, **6**, 299 (2013).
11. X. Lu, G. Li, J. Y. Kim, D. Mei, J. P. Lemmon, V. L. Sprenkle, and J. Liu, *Nat. Commun.*, **5**, 4578 (2014).
12. F. Yang, S. M. A. Mousavie, T. K. Oh, T. Yang, Y. Lu, C. Farley, R. J. Bodnar, L. Niu, R. Qiao, and Z. Li, *Adv. Energy Mater.*, **8**, 1701991 (2018).
13. G. Nikiforidis, G. J. Jongerden, E. F. Jongerden, M. C. M. van de Sanden, and M. N. Tsampas, *J. Electrochem. Soc.*, **166**, A135 (2019).
14. S. Kandhasamy, G. Nikiforidis, G. J. Jongerden, F. Jongerden, M. C. M. Sanden, and M. N. Tsampas, *ChemElectroChem*, **8**, 1156 (2021).
15. D. Wang, J. Hwang, C. Y. Chen, K. Kubota, K. Matsumoto, and R. Hagiwara, *Adv. Funct. Mater.*, **31**, 2105524 (2021).
16. K. Matsumoto, J. Hwang, S. Kaushik, C.-Y. Chen, and R. Hagiwara, *Energy Environ. Sci.*, **12**, 3247 (2019).
17. Y. Zheng, D. Wang, S. Kaushik, S. Zhang, T. Wada, J. Hwang, K. Matsumoto, and R. Hagiwara, *EnergyChem*, **4**, 100075 (2022).
18. H. Vogel, *Phys. Z.*, **22**, 645 (1921).
19. G. S. Fulcher, *J. Am. Ceram. Soc.*, **8**, 339 (1925).
20. W. Xu, E. I. Cooper, and C. A. Angell, *J. Phys. Chem. B*, **107**, 6170 (2003).
21. K. Dokko, N. Tachikawa, K. Yamauchi, M. Tsuchiya, A. Yamazaki, E. Takashima, J.-W. Park, K. Ueno, S. Seki, N. Serizawa, and M. Watanabe, *J. Electrochem. Soc.*, **160**, A1304 (2013).
22. J.-W. Park, K. Ueno, N. Tachikawa, K. Dokko, and M. Watanabe, *J. Phys. Chem. C*, **117**, 20531 (2013).
23. M. Barghamadi, A. S. Best, A. I. Bhatt, A. F. Hollenkamp, P. J. Mahon, M. Musameh, and T. Rüther, *Electrochim. Acta*, **180**, 636 (2015).